HHS Public Access

Author manuscript

Ann Biomed Eng. Author manuscript; available in PMC 2019 August 01.

Published in final edited form as:

Ann Biomed Eng. 2018 August ; 46(8): 1146–1159. doi:10.1007/s10439-018-2028-4.

Cell Mimicking Microparticles Influence the Organization, Growth, and Mechanophenotype of Stem Cell Spheroids

Nicholas R. Labriola[1], **Jessica S. Sadick**[2], **Jeffrey R. Morgan**[1,2,3], **Edith Mathiowitz**[1,2,3], and **Eric M. Darling**[1,2,3,4]

[1]Center for Biomedical Engineering, Brown University, Providence, RI

[2]Department of Molecular Pharmacology, Physiology, and Biotechnology, Brown University, Providence, RI

[3]School of Engineering, Brown University, Providence, RI

[4]Department of Orthopaedics, Brown University, Providence, RI

Abstract

Substrate stiffness is known to alter cell behavior and drive stem cell differentiation, though most research in this area has been restricted to traditional, two-dimensional (2D) culture systems rather than more physiologically relevant, three-dimensional (3D) platforms. In this study, we utilized polymer-based, cell mimicking microparticles (CMMPs) to deliver distinct, stable mechanical cues to human adipose derived stem cells (ASCs) in 3D spheroid culture to examine changes in adipogenic differentiation response and mechanophenotype. After 21 days of adipogenic induction, spheroids containing CMMPs (composite spheroids) stiffened in accordance with CMMP elasticity such that spheroids containing the stiffest, ~10 kPa, CMMPs were over 27% stiffer than those incorporating the most compliant, ~0.25 kPa CMMPs. Adipogenically induced, cell-only spheroids were over 180% larger and 50% more compliant than matched controls. Interestingly, composite spheroids cultured without chemical induction factors dissociated when presented with CMMPs stiffer than ~1 kPa, while adipogenic induction factors mitigated this behavior. Gene expression for *PPARG* and *FABP4* were upregulated more than 45-fold in adipogenically induced samples compared to controls but were unaffected by CMMP elasticity, attributed to insufficient cell-CMMP contacts throughout the composite spheroid. In summary, mechanically tuned CMMPs influenced whole-spheroid mechanophenotype and stability but minimally affected differentiation response.

Corresponding Author: Eric M. Darling, Ph.D., Brown University, 175 Meeting Street, Box G-B397, Providence, RI 02912, Phone: 401-863-6807, Fax: 401-863-7595, Eric_Darling@brown.edu.

Conflict of Interest

NRL, EM, and EMD have patent filings relevant to the technology in this study. EMD owns MimicSphere, LLC, which focuses on the same technology.

Author Contributions

NRL and EMD designed the study. NRL performed all CMMP/substrate preparation, cell culture, mechanical testing, and imaging. NRL, EMD, and JSS analyzed the data. NRL, EMD, JSS, JRM, and EM wrote and edited the manuscript. JRM and EM provided materials and consultation on the design, execution, and interpretation of the experiment and data sets.

Key terms

stem cell differentiation; adipogenesis; elastic and viscoelastic properties; 3D spheroid culture; self-assembly; atomic force microscopy (AFM); hyper-compliant microparticles; tissue engineering

Introduction

The mechanical properties of cells and the substrates they interact with are important considerations for tissue engineering applications. Substrate compliance is well-recognized to stimulate lineage-specific gene expression in stem cells.[11] Likewise, the intrinsic mechanophenotype of undifferentiated adipose-derived stem cells (ASCs) indicates a preference for lineage-specific differentiation.[14] These mechanical characteristics are interdependent as well, with recent work indicating that cellular assembly into three-dimensional (3D) nodules versus monolayers on two-dimensional (2D) substrates depends on the relative stiffness of the cell compared to its substrate.[31] By strategically selecting materials that mimic the mechanical properties of living cells and their microenvironments, improved tissue engineered constructs are possible.

Though stimulation through material compliance is accepted as having implications in cellular morphology, gene expression, and fate, research in this area has been largely restricted to 2D culture platforms, with little investigation into how these signals alter cell behavior in more complex, 3D tissues.[11, 35] Yet, 3D culture systems are considered to be more biologically relevant for tissue engineering as they better mimic in vivo microenvironments of living tissue.[1] Compliant substrate-driven stem cell differentiation in 3D has been studied via encapsulation in mechanically tuned hydrogels or porous scaffolds.[30, 38] Such research has revealed that scaffolds with reduced elasticity or crosslinking enhance adipogenic differentiation.[2, 15] However, these systems limit cell-cell interactions as they rely on either cell infiltration or isolating single cells or microtissue constructs within the mechanically tuned environment.[21, 26] Another 3D culture system, spheroid culture, involves seeding cells into a non-adherent environment to promote intercellular interactions and the self-assembly of spheroids/aggregates.[28] This method maximizes the number of cell-cell contacts formed, simplifies cell harvesting, and allows for the passive incorporation of recognizable substrates during self-assembly – all advantages over other 3D culture systems. Additionally, previous studies have reported that stem cells cultured in 3D spheroids exhibited enhanced differentiation potential compared to those cultured in 2D, providing additional motivation to optimize this technique for stem cell differentiation.[4, 6] Furthermore, the incorporation of microparticles in spheroids has been shown to improve metabolic activity and differentiation responses.[17] However, the effect of microparticle elasticity on stem cell behavior in spheroid culture has never been studied. Recently developed polyacrylamide (PAAm) cell mimicking microparticles (CMMPs), which replicate the size and elasticity of living cells, are a convenient tool for delivering stable mechanical cues to cells in 3D spheroid cultures.[22, 24]

The goal of this study was to investigate the effects of substrate stiffness on the mechanophenotype and adipogenic differentiation response of self-assembled composite

spheroids containing both ASCs and CMMPs. We hypothesized that highly compliant CMMPs would reduce whole-spheroid stiffness and enhance adipogenic differentiation, while stiffer CMMPs would yield spheroids with higher elastic moduli paired with lower levels of lineage-specific mRNA expression. To test this hypothesis, self-assembled composite spheroids containing ASCs and mechanically distinct CMMPs were maintained in either control or adipogenic induction medium for 21 days. The mechanophenotype of individual spheroids was characterized weekly using an atomic force microscope (AFM). End point assessments included the analysis of the adipogenic specific genes peroxisome proliferator-activated receptor gamma (*PPARG*) and fatty acid binding protein 4 (*FABP4*) and confocal imaging of cell-CMMP organization.

Materials and Methods

Cell Culture

ASCs were isolated from abdomen and thigh lipoaspirate of a 56-year old, female patient with a past history of breast cancer following procedures approved by the institutional review board (IRB) of Rhode Island Hospital. Tissue was processed using previously established methods [12]. Prior to experiments, ASCs were expanded to third passage in medium consisting of DMEM/F-12 (Hyclone, GE Healthcare Life Sciences, Logan, UT), 10% fetal bovine serum (FBS, ZenBio, Research Triangle Park, NC), and 1% antibiotic/animycotic (Hyclone), supplemented with 5 ng/mL epidermal growth factor, 1 ng/mL fibroblast growth factor, and 0.25 ng/mL transforming growth factor-β1 (R&D Systems, Minneapolis, MN).[13] For differentiation experiments, ASCs were exposed to either control medium containing DMEM/F-12 with 10% FBS and 1% antibiotic/antimycotic or adipogenic medium containing control medium supplemented with 0.5 μM 3-isobutyl-1-methylxanthine (IBMX), 10 μM insulin, 200 μM indomethacin, and 1 μM dexamethasone (Sigma-Aldrich, St. Louis, MO).[37] Media were changed every two days.

Preparation of Mechanically Distinct Substrates

Cell Mimicking Microparticle Fabrication—Mechanically distinct populations of CMMPs were generated through inverse emulsification using 4 or 8% acrylamide with 0.05, 0.1, 0.2, or 0.3% bis-acrylamide cross-linker (Table I), initiated with ammonium persulfate (APS) and tetramethylethylenediamine (TEMED), following previous protocols.[24] Physiologically relevant CMMP diameters were obtained using a 1500 RPM stir rate and 40 μm cell strainer. CMMPs were visualized with a rhodaminde-based dye and functionalized with a 100 μg/mL suspension of collagen-1 (Millipore, Billerica MA), via NHS-ester mediated crosslinking using 1 mg/mL sulfo-SANPAH (CovaChem, LLC, Loves Park, IL), to promote cell-CMMP interactions, as described previously.[24] The size distributions of stained CMMP populations were generated from the assessment of nine, randomly taken, 10x images using intensity thresholding and image analysis tools in Image J (U.S. National Institutions of Health, Bethesda, MD, version 1.47).

2D Gel Preparation and Coating—Two-dimensional thin gels were fabricated to match the elastic moduli of each CMMP population. Gels were formed by pipetting 75 μL of each PAAm solution (Table II) between a hydrophobic glass slide and a circular, hydrophilic glass

coverslip following previous protocols.[34] One day prior to cell seeding, gels were covalently functionalized with collagen and equilibrated in control medium.

Mechanical Characterization by AFM

The mechanical properties of individual ASCs, CMMPs, thin gels, and spheroids were characterized with an MFP-3D-BIO AFM (Asylum Research, Santa Barbara, CA) using previously described methods.[8] Samples were attached to plasma treated coverslips in 50 mm, low-profile Petri dishes with a thirty-minute incubation at 37°C and then gently flooded with 3 mL of phosphate buffered saline (PBS) or DMEM/F-12 for non-biological and biological samples, respectively. Elastic and viscoelastic properties were obtained from force vs. indentation/time curves using a modified, thin-layer Hertz model.[7, 9] Spheroid heights were determined from the difference in z-position between the initial contact when positioned over the apex of the spheroid and over the glass adjacent to where each spheroid was adhered. Data were acquired using the settings specified in Table III.

3D Spheroid Formation and 2D Culture of ASCs

To promote intercellular interactions and the self-assembly of spheroids, non-adherent microwells were fabricated from 2% molten agarose (Thermo Fisher Sci.) using 3D Petri Dish® molds (24–96-Small, Microtissues Inc., Providence, RI).[28] Microwells were cured at 4°C for 15 minutes, transferred to 24-well plates, and equilibrated in control medium for 2 days prior to introducing ASCs. Spheroids consisted of either only cells (1,200 cells) or cells mixed with one population of mechanically distinct CMMPs at a 1:1 ratio (600 cells: 600 CMMPs).

To parallel the 2D experiments reported in literature, cells were cultured on mechanically distinct PAAm gels with elastic moduli matched to the various CMMP populations. ASCs were seeded onto collagen type-1-coated coverslips or PAAm gels at 80,000 cells/well (n=3) within 24-well plates. Phase microscopy images were acquired of ASCs after 1, 10, and 21 days of culture in either adipogenic or control medium to track lipid production and morphological changes resulting from chemical and mechanical cues.

Gene Expression Analysis by Quantitative Polymerase Chain Reaction (qPCR)

To assess the adipogenic differentiation response of ASCs in 3D spheroids and on 2D gels, the expression of *PPARG* and *FABP4* was determined by qPCR after 21 days in culture. Cells/spheroids were lysed with TRIzol Reagent (Thermo Fisher Sci.), then agitated through vigorous pipetting, vortexed, and frozen at −80°C. The lysates were thawed and mRNA was isolated using QuickRNA Miniprep Kit (Zymo Research, Irvine, CA) in accordance with the manufacturer's guidelines. Isolated RNA (80 ng/reaction) was reverse transcribed using SuperScript III First Strand cDNA Synthesis Kit (Life Technologies, Waltham, MA). TaqMan Gene Expression Assay human primers (Life Technologies) for genes of interest *PPARG*, variant 2 (Hs00234592_m1), and *FABP4* (Hs01086177_m1), as well as reference gene glyceraldehyde 3-phosphate dehydrogenase (GAPDH) (Hs03929097_g1), were used in all iterations, and all samples were run in technical triplicate. Fluorescence signal denoting abundance was detected using a CFX96 Real-Time PCR Detection System (Bio-Rad,

Hercules, CA). Data were analyzed using the comparative delta Ct method,[32] with relative *PPARG* and *FABP4* expression normalized to corresponding *GAPDH* values.

Spheroid Imaging

Spheroid Formation Time-Lapse—ASCs stained with calcein AM green (1 μg/mL, AnaSpec Inc., Fremon, CA) were seeded into equilibrated agarose microwells either exclusively or with one of the mechanically distinct, rhodamine-stained, collagen-coated CMMP populations at a 1:1 ratio (115,000 total). CMMP only conditions showed no movement or self-assembly over time. A five-hour time-lapse was generated with the automatic acquisition of bright field, green-fluorescence, and red-fluorescence images at fifteen minute intervals using a Carl Zeiss Axio Observer Z1 fitted with a 20x objective, an Xcite 120 XL mercury lamp (Exfo, Life Science Division, Mississauga, Ontario), and an AxioCam MRm camera (Carl Zeiss MicroImaging, Thronwood, NY). A custom incubation chamber kept the samples at 37°C and 5% CO_2 throughout the imaging session.

Actin Staining/Confocal Imaging—Live spheroids were harvested and placed on pre-mounted coverslips within 50 mm, low-profile petri dishes (MatTek Corporation, Ashland MA) for the acquisition of confocal images. After spheroid attachment, dishes were washed three times with PBS and fixed overnight at 4°C in 10% phosphate buffered formalin (Thermo Fisher Sci.). Prior to imaging, fixed samples were rinsed thoroughly with PBS, permeabilized with a 30-minute incubation in 0.1% TritonX-100 (Sigma Aldrich) at room temperature, and stained for intracellular actin with a 30-minute incubation in 0.165 μM Alexa Fluor 488 phalloidin (Molecular Probes, Thermo Fisher Sci.). Samples were washed with PBS, and cell nuclei were subsequently stained with a 30-minute incubation in 0.1 μg/mL 4′,6-diamidino-2-phenylindole, dihydrochloride (DAPI, Molecular Probes, Thermo Fisher Sci.). To visualize cell nuclei, actin structures, and resident CMMPs, the bottom 50 μm of stained composite spheroids was imaged in 1.33 μm slices with a 40x objective on a Zeiss LSM 510 Meta Confocal Laser Scanning Microscope with an Axiovert 200M inverted microscope using Zeiss Efficient Navigation (ZEN) software version 2.1 (Carl Zeiss MicroImaging). Due to technical limitations, only half of the spheroids could be imaged using this equipment.

Statistical Analyses

To determine statistically significant differences in non-normal data sets, which included the mechanophenotype and heights of spheroid samples, two-sample Kolmogorov-Smirnov non-parametric tests were performed with R statistical analysis software version 3.31 (R Core Team 2016, Vienna, Austria). Pearson's r coefficient and p-value were calculated to determine the relationship between adipogenic composite spheroid mechanophenotype and incorporated CMMP stiffness after 21 days in culture using Microsoft Excel (2011 for Mac v.14.6.7; Microsoft Corporation, Redmond, WA). For gene expression comparisons, statistical significance was determined using a Student's T-test in Microsoft Excel. Comparisons were considered significant for p-values < 0.05. Data points more than 2.5 standard deviations from the mean were considered outliers and eliminated for all experiments. Statistical significance levels for all comparisons are presented in supplemental materials. Results and Discussion are based on interpretations using raw p-values due to the

size and scope of the study, although it should be noted this does not account for potential, type-I error introduced by multiple comparisons. For completeness, analysis using highly conservative, Holm-Bonferroni corrected p-values have been made available in Supplemental Materials.

Results

ASC, CMMP, and Gel Mechanical Characterization

Assessment of individual ASCs, CMMPs, and 2D gels with AFM confirmed physiologically relevant, yet unique, elastic moduli (Fig. 1A). Four sets of CMMPs and gels were fabricated with elastic moduli of ~0.25, ~1, ~2, and ~10 kPa, which were mechanically distinct from one another ($p < 0.0001$). The stiffest formulations were approximately an order of magnitude higher than the average ASC modulus. Average CMMP diameters were between 10–25 μm, with full distributions extending from 5–40 μm, which encompasses the typical range of mammalian cells, ~15–20μm (Fig. 1B).[18, 25]

Spheroid Temporal Mechanophenotype

Both chemical induction factors and mechanical cues induced significant temporal changes in the mechanophenotype of cell-only and composite spheroids. Initial exposure to adipogenic induction factors resulted in a rapid drop in spheroid elasticity for all CMMP conditions, such that control spheroids, on average, exhibited elastic moduli 130% higher than adipogenic spheroids by Day 1 ($p < 0.0001$; Fig. 2, Table S.I., Fig. S1–S2). After 7 days in culture, the average stiffness of all adipogenic samples increased by over 110% compared to the initial, Day 1 time point ($p < 0.004$), while controls remained unchanged ($p > 0.1$), resulting in spheroids with similar mechanophenotypes, independent of chemical induction factors ($p > 0.07$). Only ~0.25 kPa composite spheroids exhibited differences between media conditions and were 20% more compliant in adipogenic medium than control ($p < 0.02$). After the full 21-day induction period, cell-only spheroids in adipogenic media were approximately half the stiffness of paired controls ($p < 0.0001$), ~0.25 composite spheroids exhibited no difference in elasticity between medium conditions ($p > 0.3$), and adipogenic, ~1, ~2 and ~10 kPa composite spheroids were, on average, 110, 560, and 100% stiffer than paired controls, respectively ($p < 0.003$).

Within a single medium condition, no mechanophenotype differences existed in spheroids containing different CMMP populations after 1 day in culture ($p > 0.09$), with the exception of adipogenic, ~1 kPa composite spheroids, which exhibited elastic moduli that were 30% stiffer than ~0.25 kPa or cell only spheroids ($p < 0.04$). After 21 days in culture, the elasticity of adipogenic composite spheroids was positively correlated with the stiffness of incorporated CMMPs (Pearson's r coefficient = 0.37, $p < 0.005$), while no such correlation was observed for control samples (Pearson's r coefficient = 0.02, $p > 0.8$). This CMMP-based adjustment in mechanophenotype of adipogenic samples resulted in ~10 kPa composite spheroids exhibiting average elastic moduli that were 25% stiffer than ~0.25 kPa spheroids by the end of the induction period ($p < 0.03$). Additionally, adipogenic composite spheroids were 60–100% stiffer than adipogenic cell-only spheroids ($p < 0.0003$). Composite spheroids grown in the absence of chemical induction factors became unstable

and decreased in stiffness by the end of the 21-day induction period ($p < 0.05$), while cell-only spheroids in these conditions did not exhibit any changes in mechanophenotype ($p > 0.4$). Viscoelastic data were also collected and exhibited similar trends (Table S.II., Fig. S3–S6). In general, spheroid mechanical properties were distinct from either single ASCs or compliant CMMPs alone.

3D and 2D Temporal Morphologies

Spheroid heights changed temporally when presented with various chemical and mechanical cues. At the initial Day 1 time point, cell-only spheroids and composite spheroids containing ~0.25, ~1, and ~10 kPa CMMPs exhibited no differences in heights across media conditions ($p > 0.07$; Table S.I., Fig. S1–S2), while adipogenic ~2 kPa composite spheroids were 10% larger than paired control samples ($p < 0.02$). In response to chemical induction factors, cell-only spheroids continually expanded or contracted in adipogenic or control medium, respectively ($p < 0.008$, $p < 0.03$), such that cell-only control spheroids were significantly smaller than adipogenic spheroids after 21 days in culture ($p < 0.0001$). The presence of CMMPs mitigated the expansion response of adipogenic composite spheroids such that Day 1 and Day 21 samples exhibited no differences in height for any stiffness CMMP population ($p > 0.06$) and cell-only spheroids were larger than ~1, ~2, and ~10 kPa composite spheroids after 21 days ($p < 0.02$). In the absence of induction factors, composite spheroids presented with stiff CMMPs exhibited a dissociation response while hyper-compliant CMMPs prevented this behavior, such that ~10 kPa composite spheroids were significantly smaller on Day 21 than Day 1 ($p < 0.0002$), while ~0.25 kPa spheroids exhibited no temporal height differences ($p > 0.1$).

Light microscopy imaging of ASCs cultured on 2D gels revealed morphological and potential metabolic changes when grown on compliant substrates. Cells grown on ~1, ~2, and ~10 kPa gels, as well as glass coverslips, exhibited similar morphologies and intracellular lipid production (determined visually) over the 21-day induction period (Fig. 3). Cells exhibited reduced spreading on ~0.25 kPa gels and also appeared to produce lipids slightly earlier/more robustly than the samples grown on stiffer substrates. Interestingly, without induction factors present, cells cultured on ~0.25 kPa gels appeared to form spheroids/nodules.

Adipogenic Gene Expression

Expression patterns of *PPARG* and *FABP4* indicated that chemical induction factors have a much larger impact on adipogenic differentiation response than CMMP elasticity. Spheroids in adipogenic medium exhibited greater than a 45-fold increase in *PPARG* and 58,000-fold increase in *FABP4* compared to control medium ($p < 0.02$, Fig. 4, Fig. S7–S8). CMMP elasticity as a factor showed no statistical significance ($p > 0.05$). A potentially minor influence of the compliant CMMPs could be observed in the control medium conditions. For example, cell-only and ~0.25 kPa control samples both upregulated *PPARG* expression by 20% compared to ~1 kPa spheroids ($p < 0.02$). Generally, 3D control spheroids exhibited slightly higher expression of *FABP4* compared to paired, 2D samples, while the expression of *PPARG* in 3D spheroids was more than three times that of 2D monolayers for both cell-only and ~0.25 kPa control samples ($p < 0.03$).

Spheroid Assembly and CMMP Distribution

Cells successfully incorporated collagen type-I coated CMMPs into self-assembled spheroids in a passive manner (Fig. 5A). Cells appeared to initially bind to both one another and CMMPs, forming small aggregates that subsequently coalesced into a composite spheroid. Throughout the 5-hour time-lapse, cell-only spheroids appeared similar in size to composite spheroids containing coated beads. Uncoated ~1 kPa CMMPs interacted differently with cells, exhibiting one of two behaviors not observed for coated particles. Non-functionalized CMMPs were either largely excluded during assembly, suggested by the presence of red-labeled CMMPs surrounding a centralized spheroid and accumulating along the perimeter of the agarose microwells, or acted as a barrier to aggregation where cells formed smaller aggregates that did not condense into a spheroid, illustrated by both cells and CMMPs spread throughout the agarose microwells (Fig. 5B).

Confocal imaging revealed that CMMPs were largely sequestered to the center of composite spheroids after 21 days in adipogenic medium, independent of CMMP elasticity (Fig. 6). Very few cells or cell extensions were observed between CMMPs throughout the z-stacks of the spheroids. Based on limited sampling, spheroids containing ~10 kPa CMMPs exhibited increased actin cytoskeletal staining compared to those with ~0.25 or ~1 kPa CMMPs. Additionally the more compliant, ~0.25 and ~1 kPa CMMPs were noticeably deformed while ~10 kPa CMMPs maintained their spherical shapes.

Discussion

This study investigated the changes in mechanophenotype and adipogenic differentiation response of 3D ASC spheroids when presented with distinct mechanical and chemical stimuli. Time-lapse imaging illustrated that collagen-coated CMMPs are recognized by cells and that composite and cell-only spheroids self-assemble on a similar time scale into microtissue constructs of comparable diameters. After 21 days in culture, ASCs in adipogenic medium responded to CMMP elasticity by altering whole-spheroid mechanophenotype, e.g., stiffer CMMPs yielded stiffer spheroids, while composite control spheroids failed to maintain cohesive microtissues with stiffer CMMPs. Chemical induction robustly upregulated ASC adipogenic gene expression in both monolayer and spheroidal culture, while material elasticity only modestly altered the adipogenic differentiation response in either media environment. Within one day, CMMPs were sequestered to the center of composite spheroids, which limited cell-CMMP contacts and subsequent mechanical stimulation. It should be noted that this localization likely caused AFM indentation data to reflect mostly the outer shell layer of cells rather than the internalized CMMPs. This work is the first to demonstrate the self-assembly of stem cells into 3D composite spheroids with mechanically distinct microparticles incorporated as a passive, compliant element to potentially modulate mechanophenotype and differentiation response.

Time-lapse imaging of initial spheroid formation revealed that cells bind to coated CMMPs almost immediately to form small aggregates around the beads. Multiple cell-CMMP aggregates then coalesced and contracted to form a composite spheroid (Fig. 5). Notably, over the initial 5-hour formation, cell-only conditions yielded spheroids similar in size to those with CMMPs. Since total cell/microparticle number was kept constant, this suggests

that the CMMP populations of all stiffnesses were reasonable volumetric mimics of the ASC population and were incorporated at similar rates, despite a slight inverse relationship between CMMP stiffness and diameter. A previous study reported that composite spheroids generated with a 1:1 ratio of cells to particles exhibited increased cell proliferation in conditions incorporating larger particles (>100 μm) compared to those more closely matched to cell sizes (~17 μm), which maintained consistent cell numbers over a week in culture.[17] The slight size differences among CMMPs were not considered a critical characteristic for data interpretation because size differences in particles were relatively small, substantial overlap existed in the diameter distributions of all CMMP types as well as ASCs, and all stiffness particles formed similarly sized and shaped spheroids during initial formation. After the initial 5 hours of spheroid formation, cells appeared to organize towards the outskirts of the spheroid, sequestering CMMPs to the spheroid center over the next 24–48 hours. This organizational behavior was not observed in previous studies utilizing composite spheroids containing a 1:1 ratio of cells to gelatin particles with matched diameters, nor those produced using lower ratios of heterogeneously sized, fibronectin coated, PAAm particles.[10, 17] Because particles with similar sizes and ratios have not demonstrated particle aggregation within composite spheroids in previous studies, we hypothesize that this cell/CMMP organization may be due to cell action on the collagen-coated CMMPs. As the uncoated CMMPs were largely unrecognized by the cells in the current study, and fibronectin coated, PAAm particles remained dispersed in previously published work, it is unlikely that the PAAm itself is responsible for this sequestration. Altering the surface functionalization of the CMMPs with specific proteins/peptides may result in better particle distribution throughout composite spheroids.

CMMP stiffness and soluble induction factors had significant effects on whole-spheroid mechanophenotype and morphology. After 21 days in culture, the elastic moduli of adipogenically-induced ASC spheroids correlated with the stiffness of passively incorporated CMMPs. More specifically, composite spheroids containing CMMPs an order of magnitude stiffer (~10 kPa) than the average ASC were significantly stiffer than those containing hyper-compliant CMMPs (~0.25 kPa) that mimicked the low end of ASC elasticity. Since no differences in the elasticity of ~0.25 and ~10 kPa composite spheroids existed at early time points, these changes are attributed to cells responding to the elasticity of incorporated CMMPs. Additionally, in adipogenic induction medium, cell-only spheroids were more compliant and larger than any of the composite spheroid conditions. This is in good agreement with previous work, which has demonstrated that incorporating (rigid) microparticles in stem cell spheroids results in higher elastic moduli.[3] The initial introduction of soluble, adipogenic induction factors caused all spheroids to adopt a more compliant phenotype followed by a stiffening period, resulting in mechanophenotypes more similar to control spheroids after 7 days in culture. A similar initial drop in elasticity followed by stiffening has been reported in adipogenic differentiating ASCs in 2D monolayer culture,[23] suggesting that this is a real response that is conserved across both morphologies. Interestingly, when cultured without chemical induction factors, ASC spheroids became even more compliant and dissociated if CMMPs with elastic moduli greater than typical ASCs (> ~1 kPa) were incorporated, while adipogenic and control ~0.25 kPa composite spheroids exhibited no differences in mechanophenotype. The dissociation of

control spheroids containing stiffer CMMPs is hypothesized to occur as cells preferentially bind to the stiffest available substrate, in this case they bind to the CMMPs rather than other neighboring cells. As cells compete to bind to CMMPs and the two components rearrange within the spheroid, a single cell may spread across the majority of a microparticle's surface. When the cell adheres strongly enough, cell-cell connections to its neighbors are severed and the CMMP+cell may dissociate from the spheroid. After 18 days in culture, images of control composite spheroids still within the agarose microwells reveal dissociated CMMP +cell aggregates around a central cohesive spheroid when cultured with stiffer CMMPs (Fig. S9A). Select confocal images show that some of these dissociated aggregates could also bind to coverslips (Fig. S9B). The ability of cells to upregulate actin polymerization in the presence of stiffer mechanical cues can result in a stronger spreading response on stiffer CMMPs,[16] while cells presented with more compliant ~0.25 kPa substrates do not increase actin polymerization and remain more spherical with reduced spreading, resulting in more stable spheroid microtissues. This mechanosensitive response is reinforced by the 2D gel images which revealed adipogenic samples assumed spread morphologies while control samples spontaneously formed spheroids/nodules on ~0.25 kPa gels but spread on stiffer substrates. This behavior has been shown to be dependent to not only the elasticity of the substrate but also that of the cells in the system.[31] Of note, adipogenic spheroids do not dissociate with CMMPs of any stiffness, attributed to the inhibition of actin polymerization, through RhoA-ROCK signaling, caused by IBMX in the adipogenic medium.[29] It should be noted that the differences in whole-spheroid mechanophenotype of control and adipogenic composite spheroids containing either ~1, ~2 and ~10 kPa CMMPs were driven mostly by the decreased elasticity of control samples, attributed to reduced spheroid cohesiveness in these conditions. Alternative protein coatings or CMMP diameters may help mediate the dissociation response through altering the level of cell spreading. This phenomenon should be considered when delivering stiff microparticles to spheroids without additional chemical treatments and may have implications for dissociating unwanted tissue masses in more clinical applications.

The adipogenic differentiation response of ASCs was dominated by chemical induction factors, with minimal apparent effects from CMMP or gel substrate stiffness. Adipogenic medium significantly increased *PPARG* and *FABP4* expression in ASCs by 2 and 6 orders of magnitude, respectively, while material compliance induced no significant differences. Though there were few statistically significant differences in gene expression, some interesting trends did exist. Notably, ASCs had the highest relative expression for *PPARG* when grown on ~0.25 kPa, 2D gels in adipogenic medium. This suggests there could have been minor adipogenic enhancement of ASCs on the most compliant gels, though not as dramatic as reported in previous studies.[5, 11, 19] The expression of *FABP4*, which corresponds to later stages of adipogenesis, provides additional evidence of a potential mechanosensitive response as coverslips and ~10 kPa gels appeared to have slightly lower transcript levels than on ~0.25, ~1, or ~2 kPa gels without induction factors present, paralleling previous studies well.[5, 11, 19] The observation that these stiffness-dependent trends were not present in 3D control samples suggests that cells did not sense the mechanical stimuli effectively enough to alter average gene expression levels. Interestingly, cells in 3D spheroid culture generally exhibited higher adipogenic gene expression

compared to mechanically comparable 2D conditions, particularly in the absence of adipogenic induction factors. It should be noted that lysates were collected directly from agarose microwells, meaning that aggregates of cells and CMMPs surrounding dissociating spheroids were averaged into the gene expression measurements. The lack of cell-cell contacts in these instances may help explain the disconnect between the mechanophenotype of ~10 kPa control spheroids, which suggest a dissociation of the composite, and their reduced adipogenic gene expression levels, which would typically be unexpected to occur with increasing compliance. Overall, neither substrate stiffness nor culture system increased the expression levels of either *PPARG* or *FABP4* comparable to the upregulation achieved with soluble adipogenic induction factors alone.

This chemically dominated response suggests that loading CMMPs with drugs or growth factors may produce more significant enhancement in stem cell differentiation response than mechanical properties alone. As has been demonstrated with other 3D, microbead-based scaffold systems, it is possible to obtain spatial or temporal control of signals by varying amount or type of cargo loaded into CMMPs with controlled release rates that can be mixed at specific ratios.[33] The minimal effect of mechanical signals in 3D spheroids could be explained by the self-segregating behavior of CMMPs. Organizationally, most CMMPs were sequestered to the center of composite spheroids, limiting the extent of CMMP-cell contact and mechanosensing to a shell of ASCs (Fig. 5B). Interestingly, the mechanical cues provided by the 2D gels also had little effect on adipogenic gene expression, with significant upregulation only occurring in ~2 kPa samples. Substrates with elastic moduli of ~2 kPa are most similar to bulk adipose tissue and have been previously reported to induce an adipogenic differentiation response in ASCs.[36] Surprisingly, the more compliant 2D substrates did not yield the typical, rounded cell morphology reported in literature, believed to be the driving force behind upregulation of adipogenic genes without chemical induction factors present.[20] Instead, ASCs on the most compliant gels formed nodules, creating a completely different microenvironment, apparently less conducive to adipogenesis. The increased expression of *PPARG* and *FABP4* in ASC spheroids compared to paired 2D cultures, despite increased availability of soluble factors in monolayer culture, suggests that the more rounded morphology adopted by cells in spheroid cultures may promote adipogenic differentiation.[20, 27] ASCs are known to exhibit enhanced differentiation capabilities for other lineages when cultured in 3D spheroids compared to 2D monolayers.[4, 6]

In this study, collagen type-I-coated, PAAm CMMPs provided passive, stable mechanical cues to ASCs, influencing the mechanical and biological response of 3D spheroids. CMMPs mimicking the size and stiffness of ASCs allowed for normal self-assembly of spheroids with a striking core-shell arrangement of the two constituents. Composite spheroid mechanophenotype positively correlated to CMMP elasticity and was largely distinct from both the cells and CMMPs. Interestingly, spheroids containing CMMPs > ~1 kPa underwent dissociation in the absence of adipogenic induction factors, likely due to ASCs preferentially binding to stiff CMMPs over soft, neighboring cells. The most compliant, ~0.25 kPa CMMPs yielded composite spheroids with elastic moduli and heights most closely resembling the cell-only, adipogenic spheroids when cultured with or without soluble, chemical cues. This result suggests that the compliant CMMPs may induce a more

adipogenic-like mechanophenotype without requiring chemical factors. However, these low-elasticity cues yielded minimal upregulation of adipogenic-specific mRNA sequences compared to stiffer CMMP conditions in either media environment. More dramatic changes in adipogenic gene expression may arise if CMMPs were distributed homogeneously within composite spheroids throughout culture periods. Compliant CMMPs effectively modulated the mechanical and biological properties of whole spheroids without compromising the integrity of the structure, providing possibilities for the use of these cell mimics as scaffolds or mechanical dopants.

Supplementary Material

Refer to Web version on PubMed Central for supplementary material.

Acknowledgments

The authors would like to thank Manisha K. Shah for her assistance with confocal imaging. This work was supported by awards from the National Institute of General Medical Sciences (EMD, P20 GM104937), National Institute of Arthritis and Musculoskeletal and Skin Diseases (EMD, R01 AR063642), and the National Science Foundation (EMD, CAREER Award, CBET1253189). The content of this article is solely the responsibility of the authors and does not necessarily represent the official views of the National Science Foundation or National Institutes of Health.

Abbreviations, Symbols, and Terminology

AFM	atomic force microscopy
APS	ammonium persulfate
ASCs	adipose derived stem cells
CMMP	cell mimicking microparticle
$E_{elastic}$	young’s modulus/elastic modulus
E_R	relaxed modulus
E_0	instantaneous modulus
FABP4	fatty acid binding protein 4
IBMX	3-isobutyl-1-methylxanthine
PAAm	polyacrylamide
PBS	phosphate buffered saline
PPARG	peroxisome proliferator-activated receptor gamma
TEMED	tetramethylethylenediamine
μ	apparent viscosity
2D	two-dimensional

3D three-dimensional

References

1. Achilli TM, Meyer J, Morgan JR. Advances in the formation, use and understanding of multi-cellular spheroids. Expert Opinion on Biological Therapy. 2012; 12:1347–1360. [PubMed: 22784238]
2. Anderson SB, Lin CC, Kuntzler DV, Anseth KS. The performance of human mesenchymal stem cells encapsulated in cell-degradable polymer-peptide hydrogels. Biomaterials. 2011; 32:3564–3574. [PubMed: 21334063]
3. Baraniak PR, Cooke MT, Saeed R, Kinney MA, Fridley KM, McDevitt TC. Stiffening of human mesenchymal stem cell spheroid microenvironments induced by incorporation of gelatin microparticles. J Mech Behav Biomed Mater. 2012; 11:63–71. [PubMed: 22658155]
4. Baraniak PR, McDevitt TC. Scaffold-free culture of mesenchymal stem cell spheroids in suspension preserves multilineage potential. Cell and Tissue Research. 2011; 347:701–711. [PubMed: 21833761]
5. Chaudhuri O, Gu L, Klumpers D, Darnell M, Bencherif SA, Weaver JC, Huebsch N, Lee HP, Lippens E, Duda GN, Mooney DJ. Hydrogels with tunable stress relaxation regulate stem cell fate and activity. Nat Mater. 2016; 15:326–334. [PubMed: 26618884]
6. Cheng NC, Chen SY, Li JR, Young TH. Short-term spheroid formation enhances the regenerative capacity of adipose-derived stem cells by promoting stemness, angiogenesis, and chemotaxis. Stem Cells Translational Medicine. 2013; 2:584–594. [PubMed: 23847001]
7. Darling EM, Zauscher S, Block JA, Guilak F. A thin-layer model for viscoelastic, stress-relaxation testing of cells using atomic force microscopy: do cell properties reflect metastatic potential? Biophys J. 2007; 92:1784–1791. [PubMed: 17158567]
8. Darling EM, Zauscher S, Guilak F. Viscoelastic properties of zonal articular chondrocytes measured by atomic force microscopy. Osteoarthritis and Cartilage. 2006; 14:571–579. [PubMed: 16478668]
9. Dimitriadis EK, Horkay F, Maresca J, Kachar B, Chadwick RS. Determination of elastic moduli of thin layers of soft material using the atomic force microscope. Biophysical Journal. 2002; 82:2798–2810. [PubMed: 11964265]
10. Dolega ME, Delarue M, Ingremeau F, Prost J, Delon A, Cappello G. Cell-like pressure sensors reveal increase of mechanical stress towards the core of multicellular spheroids under compression. Nat Commun. 2017; 8:14056. [PubMed: 28128198]
11. Engler AJ, Sen S, Sweeney HL, Discher DE. Matrix elasticity directs stem cell lineage specification. Cell. 2006; 126:677–689. [PubMed: 16923388]
12. Estes BT, Diekman BO, Gimble JM, Guilak F. Isolation of adipose-derived stem cells and their induction to a chondrogenic phenotype. Nature Protocols. 2010; 5:1294–1311. [PubMed: 20595958]
13. Estes BT, Diekman BO, Guilak F. Monolayer cell expansion conditions affect the chondrogenic potential of adipose-derived stem cells. Biotechnology and Bioengineering. 2008; 99:986–995. [PubMed: 17929321]
14. Gonzalez-Cruz RD V, Fonseca C, Darling EM. Cellular mechanical properties reflect the differentiation potential of adipose-derived mesenchymal stem cells. Proceedings of the National Academy of Sciences. 2012; 109:E1523–E1529.
15. Guneta V, Loh QL, Choong C. Cell-secreted extracellular matrix formation and differentiation of adipose-derived stem cells in 3D alginate scaffolds with tunable properties. J Biomed Mater Res A. 2016; 104:1090–1101. [PubMed: 26749566]
16. Guo WH, Frey MT, Burnham NA, Wang YL. Substrate rigidity regulates the formation and maintenance of tissues. Biophys J. 2006; 90:2213–2220. [PubMed: 16387786]
17. Hayashi K, Tabata Y. Preparation of stem cell aggregates with gelatin microspheres to enhance biological functions. Acta Biomaterialia. 2011; 7:2797–2803. [PubMed: 21549223]
18. Hielscher AH, Mourant JR, Bigio IJ. Influence of particle size and concentration on the diffuse backscattering of polarized light from tissue phantoms and biological cell suspensions. Applied Optics. 1997; 36:125–135. [PubMed: 18250653]

19. Huebsch N, Arany PR, Mao AS, Shvartsman D, Ali OA, Bencherif SA, Rivera-Feliciano J, Mooney DJ. Harnessing traction-mediated manipulation of the cell/matrix interface to control stem-cell fate. Nat Mater. 2010; 9:518–526. [PubMed: 20418863]
20. Kilian KA, Bugarija B, Lahn BT, Mrksich M. Geometric cues for directing the differentiation of mesenchymal stem cells. Proceedings of the National Academy of Sciences. 2010; 107:4872–4877.
21. Kumachev A, Greener J, Tumarkin E, Eiser E, Zandstra PW, Kumacheva E. High-throughput generation of hydrogel microbeads with varying elasticity for cell encapsulation. Biomaterials. 2011; 32:1477–1483. [PubMed: 21095000]
22. Labriola NR, Azagury A, Gutierrez R, Mathiowitz E, Darling EM. Concise Review: Fabrication, customization, and application of cell mimicking microparticles in stem cell science. Stem Cells Transl Med. 2018; 7:232–240. [PubMed: 29316362]
23. Labriola NR, Darling EM. Temporal heterogeneity in single-cell gene expression and mechanical properties during adipogenic differentiation. J Biomech. 2015; 48:1058–1066. [PubMed: 25683518]
24. Labriola NR, Mathiowitz E, Darling EM. Fabricating polyacrylamide microbeads by inverse emulsification to mimic the size and elasticity of living cells. Biomater Sci. 2017; 5:41–45.
25. Lo Surdo J, Bauer SR. Quantitative approaches to detect donor and passage differences in adipogenic potential and clonogenicity in human bone marrow-derived mesenchymal stem cells. Tissue Eng Part C Methods. 2012; 18:877–889. [PubMed: 22563812]
26. Loh QL, Choong C. Three-dimensional scaffolds for tissue engineering applications: Role of porosity and pore size. Tissue Engineering Part B: Reviews. 2013; 19:485–502. [PubMed: 23672709]
27. McBeath R, Pirone DM, Nelson CM, Bhadriraju K, Chen CS. Cell shape, cytoskeletal tension, and RhoA regulate stem cell lineage commitment. Developmental Cell. 2004; 6:483–495. [PubMed: 15068789]
28. Napolitano A, Dean D, Man A, Youssef J, Ho D, Rago A, Lech M, Morgan J. Scaffold-free three-dimensional cell culture utilizing micromolded nonadhesive hydrogels. BioTechniques. 2007; 43:494–500. [PubMed: 18019341]
29. Nobusue H, Onishi N, Shimizu T, Sugihara E, Oki Y, Sumikawa Y, Chiyoda T, Akashi K, Saya H, Kano K. Regulation of MKL1 via actin cytoskeleton dynamics drives adipocyte differentiation. Nature Communications. 2014; 5
30. Parekh SH, Chatterjee K, Lin-Gibson S, Moore NM, Cicerone MT, Young MF, Simon CG Jr. Modulus-driven differentiation of marrow stromal cells in 3D scaffolds that is independent of myosin-based cytoskeletal tension. Biomaterials. 2011; 32:2256–2264. [PubMed: 21176956]
31. Shah MK I, Garcia-Pak H, Darling EM. Influence of inherent mechanophenotype on competitive cellular adherence. Ann Biomed Eng. 2017; 45:2036–2046. [PubMed: 28447179]
32. Silver N, Best S, Jiang J, Thein S. Selection of housekeeping genes for gene expression studies in human reticulocytes using real-time PCR. BMC Molecular Biology. 2006; 7:33. [PubMed: 17026756]
33. Singh M, Morris CP, Ellis RJ, Detamore MS, Berkland C. Microsphere-based seamless scaffolds containing macroscopic gradients of encapsulated factors for tissue engineering. Tissue Eng Part C. 2008; 14:299–309.
34. Tse JR, Engler AJ. Preparation of hydrogel substrates with tunable mechanical properties. Curr Protoc Cell Biol. 2010; Chapter 10(Unit 10):16.
35. Yeung T, Georges PC, Flanagan LA, Marg B, Ortiz M, Funaki M, Zahir N, Ming W, Weaver V, Janmey PA. Effects of substrate stiffness on cell morphology, cytoskeletal structure, and adhesion. Cell Motility and the Cytoskeleton. 2005; 60:24–34. [PubMed: 15573414]
36. Young DA, Choi YS, Engler AJ, Christman KL. Stimulation of adipogenesis of adult adipose-derived stem cells using substrates that mimic the stiffness of adipose tissue. Biomaterials. 2013; 34:8581–8588. [PubMed: 23953825]
37. Zheng B, Cao B, Li G, Huard J. Mouse adipose-derived stem cells undergo multilineage differentiation in vitro but primarily osteogenic and chondrogenic differentiation in vivo. Tissue Engineering. 2006; 12:1891–1901. [PubMed: 16889519]

38. Zoldan J, Karagiannis ED, Lee CY, Anderson DG, Langer R, Levenberg S. The influence of scaffold elasticity on germ layer specification of human embryonic stem cells. Biomaterials. 2011; 32:9612–9621. [PubMed: 21963156]

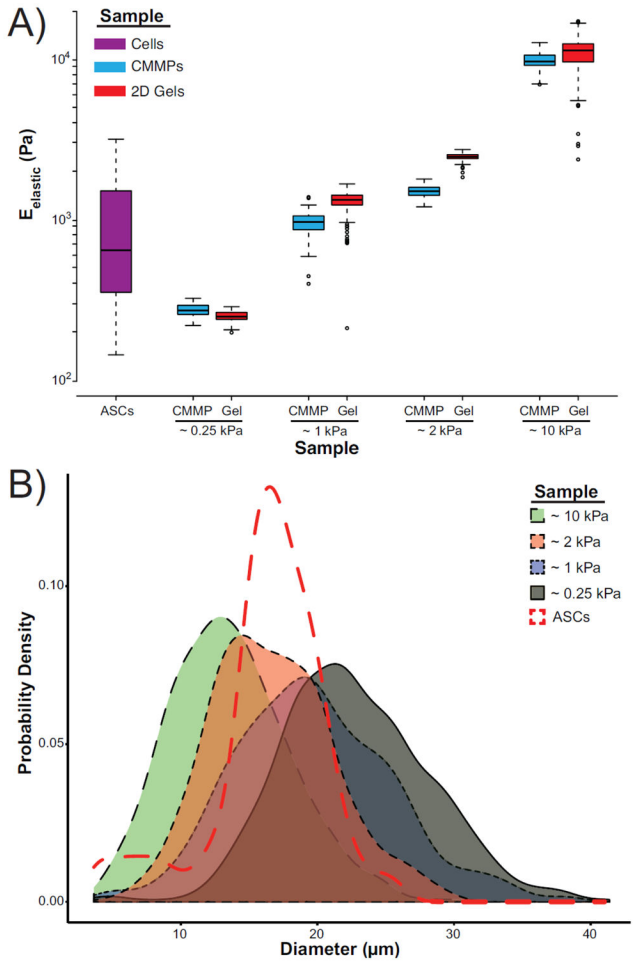

Figure 1. ASC, CMMP, and thin gel characterization

(A) Box and whisker plots represent the distribution of $E_{elastic}$ for human ASCs (purple) as well as the four CMMP formulations (blue) and their paired, thin gels (red). The three most compliant CMMP formulations fall within the ASC range while the final formulation is approximately an order of magnitude stiffer than the cells. (B) Probability density plots illustrate the distribution of microparticle diameters for each polyacrylamide formulation: ~0.25 kPa (grey), ~1 kPa (blue), ~2 kPa (red), and ~10 kPa (green). The size distributions of all populations overlap the typical size of mammalian cells (5–50 μm). The probability density plot of the ASCs used in this study is illustrated by the red dotted line.

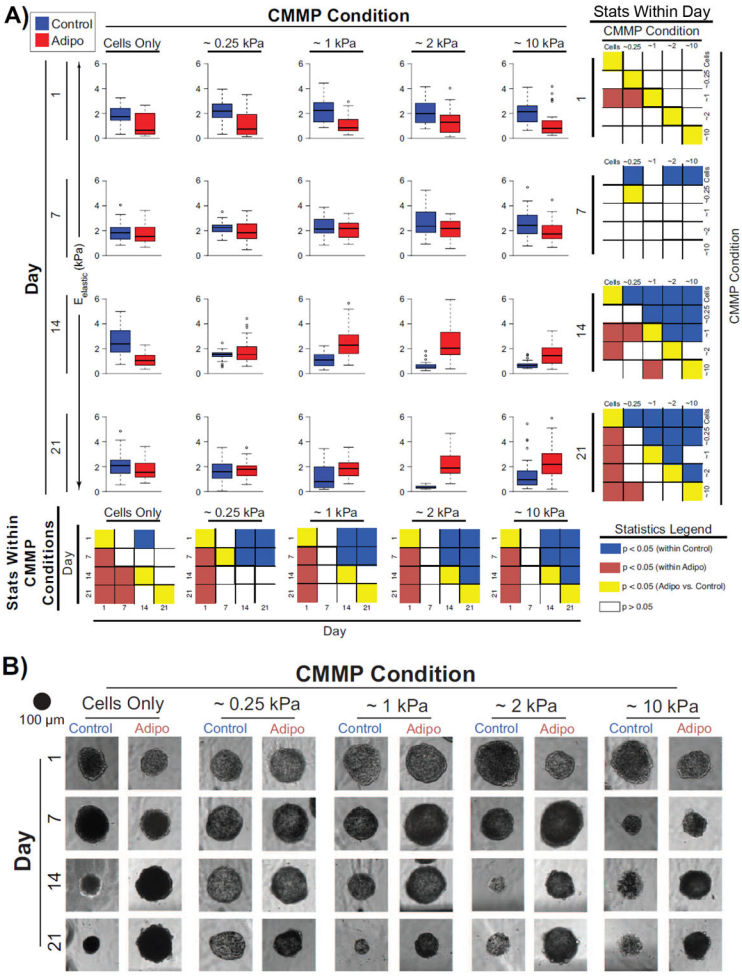

Figure 2. Temporal changes in composite spheroid elasticities and heights

(A) Box plots of adipogenic (red) and control (blue) spheroid elastic moduli, $E_{elastic}$, and (B) matched, representative, bright field images are displayed in a matrix where descending rows illustrate later time points and columns represent increasing stiffness of incorporated CMMPs from left to right. For box plots, the blue (control) and red (adipogenic) colored regions represent the 25–75% quartile ranges, the central black line represents the median of the data, and the whiskers represent the data with outliers (circles) removed. The smaller matrices at the end of each row and column depict the statistical comparisons using raw p-values across CMMP conditions and day, respectively. Significant differences within either control or adipogenic groups are represented by blue and red boxes, respectively. Differences across media environments are denoted by yellow boxes, while comparisons that were not significantly different are represented by white boxes.

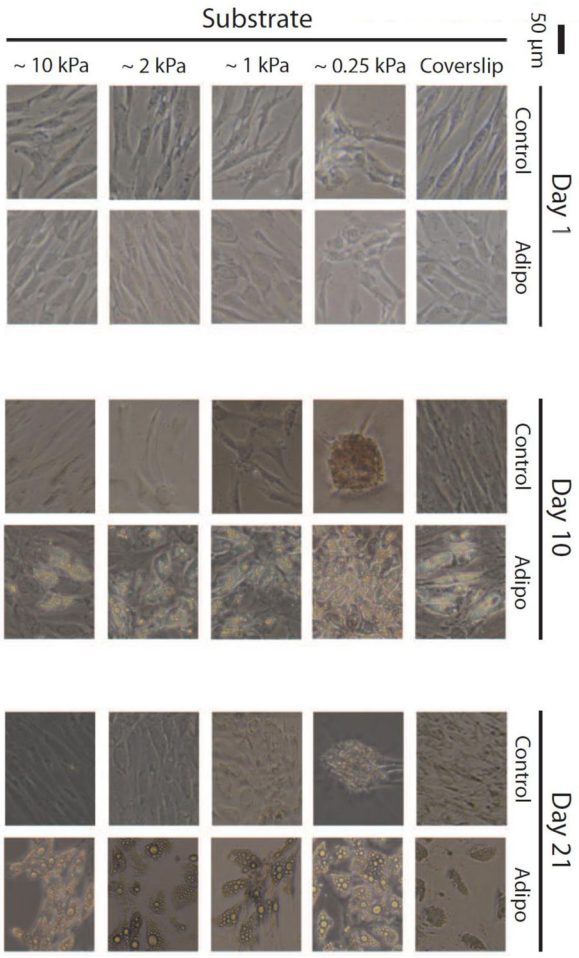

Figure 3. Two-dimensional imaging of ASCs on matched, compliant gels

Phase contrast images depict ASCs after 1, 10, and 21 days in either control or adipogenic medium on coverslips or ~0.25, ~1, ~2, or ~10 kPa PAAm gels. Induced ASCs produced visible lipids after 10 days, with the most dramatic response occurring on the most compliant gel. After 21 days, lipids droplets increased in diameter with less noticeable differences among the substrates. Nodule formation was apparent for control ASCs on the most compliant gels.

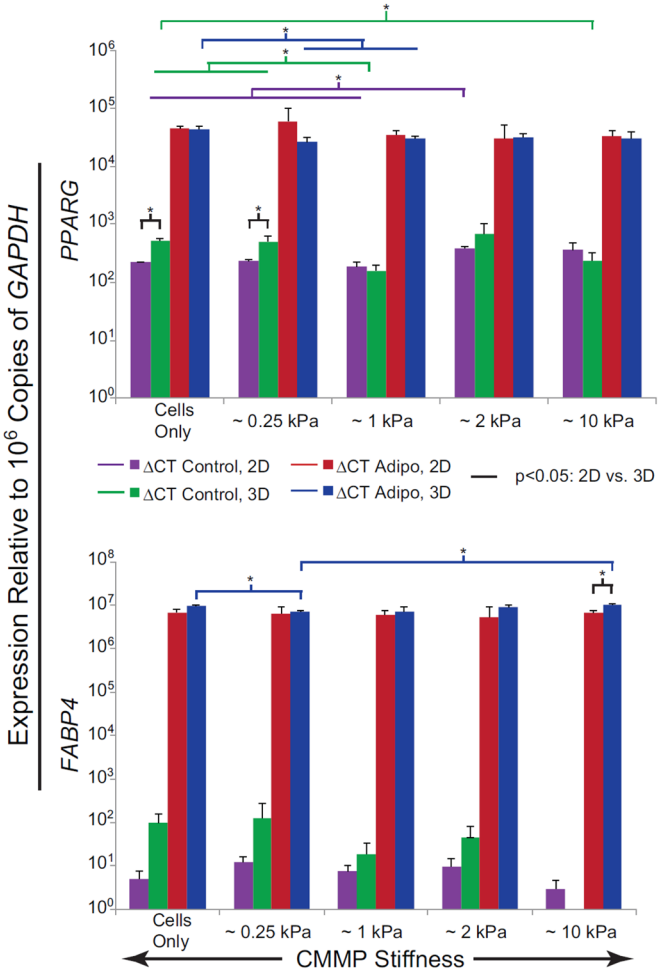

Figure 4. Adipogenic gene expression of ASCs after 21 days of exposure to mechanical cues in 2D and 3D, both with and without chemical induction

Bar graphs illustrate the expression of *PPARG* (top) and *FABP4* (bottom) of ASCs after 21 days of culture in either adipogenic or control medium environments. Colored bars indicate comparisons with p-values < 0.05 between 2D and 3D culture systems (black), 3D adipogenic samples (blue), 2D adipogenic samples (red), 3D control samples (green), and 2D control samples (purple).

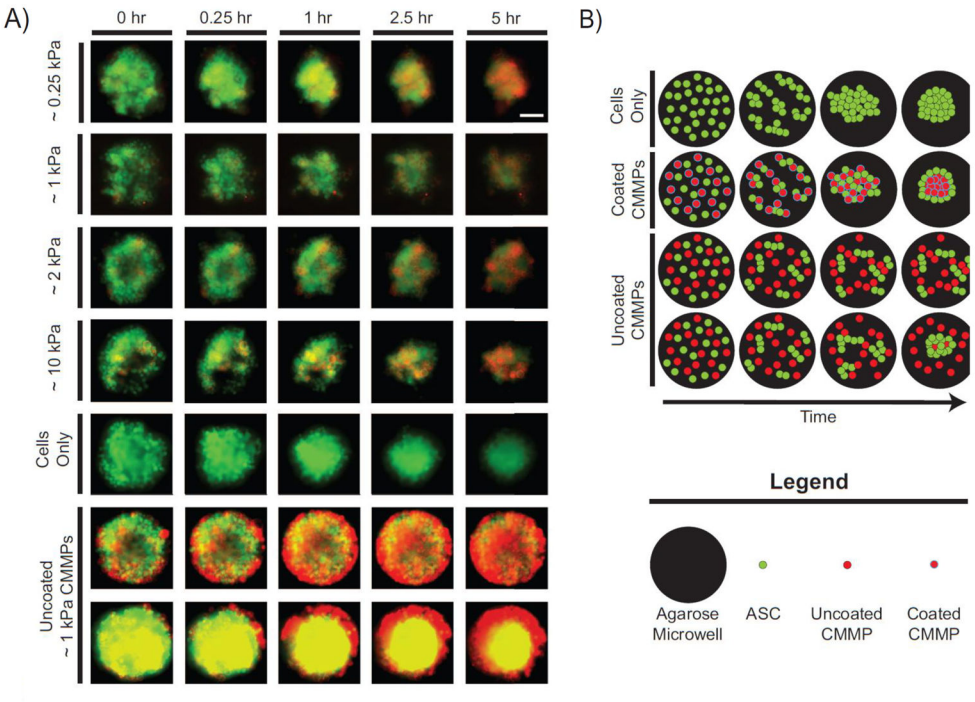

Figure 5. Composite spheroid formation during initial 5 hrs

(A) Human ASCs (green) recognized collagen type-I-coated CMMPs (red) of varying elastic moduli (~0.25 kPa, ~1 kPa, ~2 kPa, ~10 kPa) and successfully formed composite spheroids. Using ~1 kPa as a representative case, cells did not recognize uncoated microbeads and either formed small aggregates, remained separates with CMMPs acting as barriers, or formed cell-only spheroids, excluding the majority of CMMPs. Cell-only spheroids were roughly the same size as the composite spheroids. Columns from left to right illustrate increasing time from t=0, which was approximately 15–20 minutes after the first well was seeded with cells, while rows represent CMMP sample groups. Yellow coloring represents co-localization of red and green signals and the scale bar represents 100 μm. (B) This cartoon illustrates a simplified depiction of spheroid assembly for cells (green) alone as well as with coated or uncoated CMMPs (red with blue and black outlines, respectively).

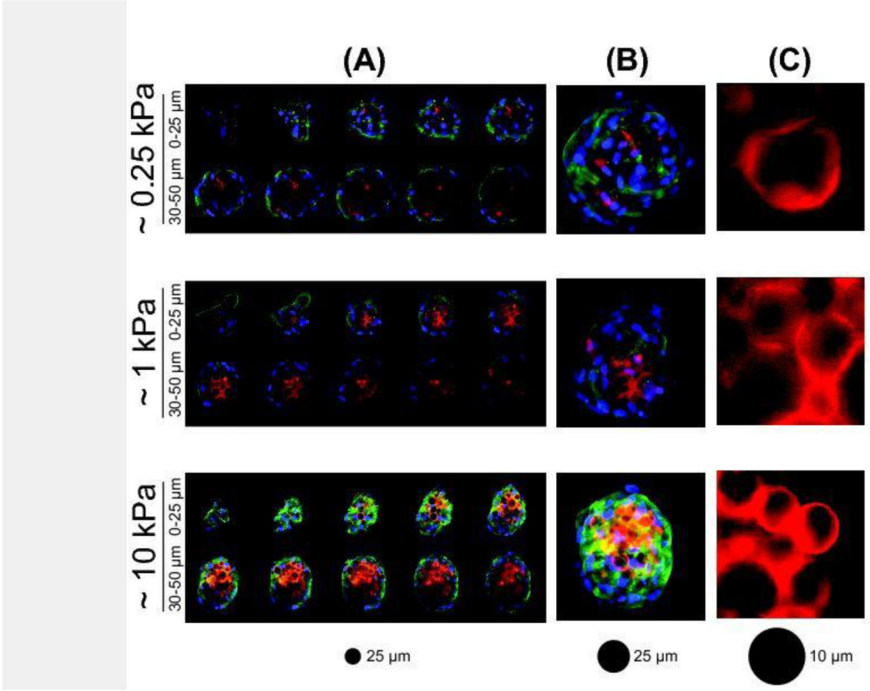

Figure 6. Confocal images of composite spheroids and CMMP deformation after 21 days of adipogenic induction

Composite spheroids containing ~0.25, ~1, and ~10 kPa CMMPs self-segregated in a consistent manner. Cell nuclei (blue) were stained with DAPI, actin cytoskeletal structures (green) with phalloidin, and CMMPs (red) with rhodamine. Illustrated here are (A) representative z-stacks of the first 50 μm in 5 μm steps, (B) 3D projections of the z-stacks, and (C) isolated regions of CMMPs illustrating deformation differences.

Table I

CMMP formulations

		Target Stiffness Acry%/Bis%			
		~0.25 kPa 4%/0.05%	**~1 kPa 4%/0.1%**	**~2 kPa 4%/0.2%**	**~10 kPa 8%/0.3%**
PAAm Solution Components	Acrylamide (mL)	1.0	1.0	1.0	2.0
	Bis-acrylamide (mL)	0.25	0.5	1.0	1.5
	10% APS (mL)	0.1	0.1	0.1	0.1
	TEMED (mL)	0.01	0.01	0.01	0.01
	PBS (mL)	8.64	8.39	7.89	6.39
Measured Characteristics	Height (μm)	22.1 ± 5.4	18.8 ± 5.8	16.1 ± 4.5	12.9 ± 4.4
	$E_{elastic}$ (kPa)	0.27 ± 0.03	0.94 ± 0.19	1.51 ± 0.13	9.74 ± 1.36

Table II

Thin gel formulations

		Target Stiffness Acry%/Bis%			
		~0.25 kPa 4%/0.06%	**~1 kPa 4%/0.09%**	**~2 kPa 4%/0.15%**	**~10 kPa 8%/0.28%**
PAAm Solution Components	Acrylamide (mL)	1.0	1.0	1.0	2.0
	Bis-acrylamide (mL)	0.3	0.45	0.75	1.4
	10% APS (mL)	0.1	0.1	0.1	0.1
	TEMED (mL)	0.01	0.01	0.01	0.01
	PBS (mL)	8.59	8.44	8.14	6.49
Measured Stiffness	$E_{elastic}$ (kPa)	0.25 ± 0.02	1.26 ± 0.24	2.48 ± 0.14	10.60 ± 3.19

Table III

AFM testing conditions

Sample	Sample Size (n)	Measured Properties	Nominal Cantilever Stiffness (N/m)	Cantilever Tip Diameter (μm)	Approach Velocity (μm/s)	Trigger Force (nN)	Region Probed
ASCs	22	elastic/viscoelastic	0.03	5	10	3	peri-nuclear
CMMPs	47–51	elastic	0.03	5	10	3	apex
Thin Gels	105–106	elastic	0.03	5	10	3	90 × 90 μm square
Spheroids (By Day)	D0: 20–36 D7: 30–36 D14: 22–32 D21: 5–21	elastic/viscoelastic	0.35	25	10	30	apex